

# A hybrid classical-quantum algorithm for digital image processing

Alok Shukla<sup>1</sup> and Prakash Vedula<sup>2</sup>

<sup>1</sup>School of Arts and Sciences, Ahmedabad University, India

<sup>1</sup>alok.shukla@ahduni.edu.in

<sup>2</sup>School of Aerospace and Mechanical Engineering, University of Oklahoma, USA

<sup>2</sup>pvedula@ou.edu

December 26, 2022

## Abstract

A hybrid classical-quantum approach for evaluation of multi-dimensional Walsh-Hadamard transforms and its applications to quantum image processing are proposed. In this approach, multidimensional Walsh-Hadamard transforms are obtained using quantum Hadamard gates (along with state-preparation, shifting, scaling and measurement operations). The proposed approach for evaluation of multidimensional Walsh-Hadamard transform has a considerably lower computational complexity (involving  $O(N^d)$  operations) in contrast to classical Fast Walsh-Hadamard transform (involving  $O(N^d \log_2 N^d)$  operations), where  $d$  and  $N$  denote the number of dimensions and degrees of freedom along each dimension. Unlike many other quantum image representation and quantum image processing frameworks, our proposed approach makes efficient use of qubits, where only  $\log_2 N$  qubits are sufficient for sequential processing of an image of  $N \times N$  pixels. Selected applications of the proposed approach (for  $d = 2$ ) are demonstrated via computational examples relevant to basic image filtering and periodic banding noise removal and the results were found to be satisfactory.

## 1 Introduction

The benefits of quantum computing algorithms over their classical counterparts have been demonstrated in the literature in several areas, including those relevant to factorization of large integers (via Shor's algorithm [1, 2]), searching of an unstructured database for the marked entry (via Grover's algorithm [3, 4] based on amplitude amplification), solutions of systems of linear equations [5] and systems of linear ordinary differential equations [6], solution of graph theory problems (based on a hybrid classical quantum algorithm known as the Quantum Approximate Optimization Algorithm [7]), solution of nonlinear differential equations [8] and machine learning [9].

Quantum algorithms have also been shown to offer considerable advantages in certain aspects of image processing (e.g. edge detection, pattern matching and recognition) [10, 11, 12, 13]. A number of quantum image representations have been proposed and surveyed in Ref. [14]. Some commonly considered quantum image representation formats include qudit lattice, FQRI, NEQR, QPIE or Real Ket [15, 12, 11].

In the following, we will compare a few key features of our proposed approach with some of the existing quantum image processing frameworks.

We note that for representation of a classical image of  $N \times N$  pixels, the Real Ket format has a high storage efficiency as it just needs  $2 \log_2 N$  qubits to represent the image, while FQRI and qudit lattice require  $N^2$  and  $2 \log_2 N + 1$  qubits respectively. For instance, in the original Real Ket representation, the probability amplitudes correspond to normalized gray level values, where the normalization factor is constructed based on all pixel values in the image. In our proposed work, we use a new hybrid classical-quantum approach for image processing. The image is represented classically and only  $\log_2 N$  qubits are sufficient at any time for row/column based sequential processing of an image of  $N \times N$  pixels (see Remark 4.0.1). Here probability amplitudes correspond to normalized gray level values of each row (or column), where the normalization factor is constructed according the pixel values in each row (or column) of the image. The requirement of fewer qubits ( $\log_2 N$ ) in the proposed approach makes it more efficient than the original Real Ket representation (using  $2 \log_2 N$  qubits) and many other existing quantum image representation and processing frameworks [12]), especially in view of the limitations of capacity (i.e. number of qubits available), cost and measurement challenges (associated with handling of multiple qubits). The proposed representation will also be useful in the context of parallel computing (where each processor is tasked with handling rows (or columns) of data).

For image filtering applications, we consider image representations in Walsh-Hadamard basis functions. Our choice of basis functions is primarily guided by the natural connection between the Walsh-Hadamard transform [16] and the Hadamard gate [17] that is widely used in many quantum circuits and algorithms. Further we note that Walsh-Hadamard basis functions are already being used in classical image processing applications [18]. Such basis functions and associated transforms have also been found to be useful in several other fields, for example, signal processing [19], solution of non-linear differential equations [20, 21], solution of partial differential equations relevant to fluid dynamics [22, 23, 24], solution of variational problems [25], and cryptography [26].

The authors recently proposed a hybrid classical-quantum approach for obtaining Walsh-Hadamard transforms of arbitrary vectors [8] and applied it to solution of nonlinear ordinary differential equations. In particular, in Ref. [8], the authors showed how useful classical information could be extracted using quantum Hadamard gates and the approach presented therein. Note that this approach primarily involves a combination of state preparation, shifting, scaling and measurement operations. It was shown that the hybrid classical-quantum approach for Walsh-Hadamard transform proposed in Ref. [8] has significantly lower computational complexity ( $\mathcal{O}(N)$  operations) in comparison to the classical Fast Walsh-Hadamard transform ( $\mathcal{O}(N \log_2 N)$  operations).

While the authors' previous work [8] demonstrated a hybrid classical-quantum approach for evaluation of one-dimensional Walsh-Hadamard transforms, the present work is focused on extensions to evaluation of multi-dimensional Walsh-Hadamard transforms (using a hybrid classical-quantum approach) and applications to image processing. In the two-dimensional case, relevant to image processing, the proposed hybrid approach has a computational complexity of  $O(N_1 N_2)$  for computing the two-dimensional Walsh-Hadamard transform of an  $N_1 \times N_2$  matrix (where  $N_1$  and  $N_2$  are powers of 2) containing image data. In contrast, for obtaining the same result, the classical two-dimensional fast Walsh-Hadamard transform has a computational complexity of  $O(N_1 N_2 \log_2(N_1 N_2))$ . Applications of the proposed hybrid approach for two-dimensional Walsh-Hadamard transforms are demonstrated through computational examples relevant to image filtering. More generally, we show that the computational complexity of the proposed

approach for the computation of a multi-dimensional Walsh-Hadamard transform, as defined in Eq. (4.4), is much lower with  $\mathcal{O}\left(\prod_{k=1}^d N_k\right)$  operations compared to the classical Fast Walsh-Hadamard transform that needs  $\mathcal{O}\left(\prod_{k=1}^d N_k \log_2\left(\prod_{k=1}^d N_k\right)\right)$  operations.

The rest of this paper is organized as follows. In section 2, we present some basic definitions and properties of the classical Walsh-Hadamard transform and its quantum analog (implemented via the use of quantum Hadamard gates). A discussion of a hybrid classical-quantum approach for a one-dimensional Walsh-Hadamard transform is included in section 3. Proposed extension of this hybrid approach to two-dimensional (and multi-dimensional) Walsh-Hadamard transforms, is presented in section 4. In section 5, applications of the proposed hybrid classical-quantum approach for two-dimensional Walsh-Hadamard transforms, in the context of image processing, are demonstrated using computational examples relevant to basic image filtering and periodic banding noise removal. Conclusions are summarized in section 6.

## 2 Walsh-Hadamard Transform

Throughout this paper we will use the convention that  $x_i \in \{0,1\}$  will denote the  $i$ -th bit in the binary representation of the integer  $x$ . More explicitly, it means, if  $x = x_0 + x_1 2 + x_2 2^2 + \dots + x_i 2^i + \dots + x_{n-1} 2^{n-1}$ , then  $x_i$  is the  $i$ -th bit in the binary representation of  $x$ .

**Definition 2.0.1.** Let  $\mathbf{v} = [f(0) \ f(1) \ f(2) \ \dots \ f(N-1)]^T$  be a vector with  $N = 2^n$  components. Then its Walsh-Hadamard transform is the vector  $\widehat{\mathbf{v}} = [\widehat{f}(0) \ \widehat{f}(1) \ \widehat{f}(2) \ \dots \ \widehat{f}(N-1)]^T$ , where for  $k = 0, 1, 2, \dots, N-1$ , the component  $\widehat{f}(k)$  of  $\widehat{\mathbf{v}}$  is defined by

$$\widehat{f}(k) = \frac{1}{\sqrt{N}} \sum_{m=0}^{N-1} f(m) (-1)^{\sum_{i=0}^{n-1} m_i k_i}. \quad (2.1)$$

Here,  $k_i$  and  $m_i$  are the  $i$ -th bits in the binary representations of  $k$  and  $m$ , respectively. Similarly, given  $\widehat{\mathbf{v}}$ , its inverse Walsh-Hadamard transform is  $\mathbf{v}$  such that the component  $f(m)$  of  $\mathbf{v}$  is defined by

$$f(m) = \frac{1}{\sqrt{N}} \sum_{k=0}^{N-1} \widehat{f}(k) (-1)^{\sum_{i=0}^{n-1} m_i k_i}. \quad (2.2)$$

We will write

$$[f(0) \ f(1) \ f(2) \ \dots \ f(N-1)]^T \longleftrightarrow [\widehat{f}(0) \ \widehat{f}(1) \ \widehat{f}(2) \ \dots \ \widehat{f}(N-1)]^T$$

to denote the pair of a vector and its Walsh-Hadamard transform.

Alternatively, for any integer  $N = 2^n$ , the Walsh-Hadamard transform of the given vector

$$\mathbf{v} = [f(0) \ f(1) \ \dots \ f(N-1)]^T$$

may be obtained by computing

$$(H^{\otimes n} \mathbf{v}), \quad (2.3)$$

where

$$H = \frac{1}{\sqrt{2}} \begin{pmatrix} 1 & 1 \\ 1 & -1 \end{pmatrix}. \quad (2.4)$$

A naive approach to compute the Walsh-Hadamard transform involving the above matrix-vector multiplication is of the order  $\mathcal{O}(N^2)$  where  $N = 2^n$ . Although, a faster classical algorithm, namely the Fast Walsh-Hadamard Transform [27], [16] exists. The classical Fast Walsh-Hadamard Transform algorithm has the time complexity of the order of  $\mathcal{O}(N \log_2 N)$  for computing the Walsh-Hadamard transform of an input vector of size  $N = 2^n$ .

## 2.1 Quantum Walsh-Hadamard Transform

We note that the matrix  $H$  in Eq. (2.3) is the transformation matrix of the quantum Hadamard gate in a computational basis. Let  $N = 2^n$  and  $\mathbf{v} = [f(0) \ f(1) \ f(2) \ \dots \ f(N-1)]^T$  be a normalized vector, i.e.,  $\|\mathbf{v}\| = 1$ , or equivalently,  $\sum_{k=0}^{N-1} (f(k))^2 = 1$ . We note that the quantum implementation of Walsh-Hadamard transform of  $\mathbf{v}$  involves preparing the initial state  $\sum_{k=0}^{N-1} f(k)|k\rangle$ , and then applying quantum Hadamard gates  $H^{\otimes n}$  on it. It can be verified that,

$$H^{\otimes n} \left[ \sum_{k=0}^{N-1} f(k)|k\rangle \right] = \frac{1}{\sqrt{N}} \sum_{k=0}^{N-1} \left( \sum_{m=0}^{N-1} f(m)(-1)^{\sum_{i=0}^{n-1} m_i k_i} \right) |k\rangle = \sum_{k=0}^{N-1} \widehat{f}(k) |k\rangle.$$

## 3 Hybrid Classical-Quantum Approach for Walsh-Hadamard Transform

A thoughtful adaptation of the quantum Walsh-Hadamard transform is central to our approach to image processing applications. The Hadamard gate is one of the most useful quantum gates. One can find the Walsh-Hadamard transform to be the first step in many important quantum algorithms. It was discussed earlier that the Walsh-Hadamard transform of  $\mathbf{v} = [f(0) \ f(1) \ \dots \ f(N-1)]^T$  is given by  $(H^{\otimes n} \mathbf{v})$ . Assuming that  $\|\mathbf{v}\| = 1$ , a simple quantum circuit consisting of  $n$  Hadamard gates can compute the Walsh-Hadamard transform of an input vector  $\mathbf{v}$  of size  $N = 2^n$ . However, the difficulty in this simple approach lies in the measurement. One can only find the square of the amplitudes of the Walsh-Hadamard transform values by carrying out the measurement. As the input sequence is assumed to be real, the components of Walsh-Hadamard transformed vector  $\widehat{\mathbf{v}}$  would also be real. However, the components of  $\widehat{\mathbf{v}}$  may be positive or negative and this sign information is lost on carrying out the measurement. We note that for many image processing applications the pixel values may be non-negative. For example, for gray scale representation the pixel values may vary from 0 to 255. However, application of the Walsh-Hadamard transforms of row/column vectors may result in vectors that contain negative values. This could potentially present challenges in unambiguous measurement as described earlier.

We tackled the core problem of obtaining Walsh-Hadamard transforms with the correct sign information in reference [8], by exploiting the structure of the Walsh-Hadamard transform matrix. The approach in [8] depended upon a key lemma (see Lemma 4.0.1 in [8]). This resulted in an algorithm of  $\mathcal{O}(N)$  (See Algorithm 1 in [8]) to compute the Walsh-Hadamard transform of an input vector of size  $N$ . We reproduce

Algorithm 1 in [8] in the following for easy reference.

---

**Algorithm 1:** A hybrid classical-quantum algorithm for computing the Walsh-Hadamard transform  $\mathcal{H}_Q(A)$  (in the sequency order) of a given input vector  $A$ .

---

**Input:** The input vector  $A = [a_0 \ a_1 \ a_2 \ \dots \ a_{N-1}]^T$  where  $N = 2^n$  is a positive integer and  $a_i \in \mathbb{R}$  for  $i = 0$  to  $i = N - 1$ .

**Output:** The Walsh-Hadamard transform (in the sequency order) of the input vector.

```

1 Function  $\mathcal{H}_Q(A)$ 
2    $b_0 = \epsilon + \sum_{k=0}^{N-1} |a_k|$  // Here  $\epsilon$  is any positive number.
3    $c = \sqrt{b_0^2 + \sum_{k=1}^{N-1} a_k^2}$  // Let  $\tilde{A} = [b_0 \ a_1 \ a_2, \dots \ a_{N-1}]^T$ . Then  $c = \|\tilde{A}\|$ .
4   Prepare the state  $|\Psi\rangle = \frac{b_0}{c} |0\rangle + \sum_{k=1}^{N-1} \frac{a_k}{c} |k\rangle$  using  $n$  qubits. // Initialize the state  $|\Psi\rangle$  with  $\frac{\tilde{A}}{\|\tilde{A}\|}$ .
5   Apply  $H^{\otimes n}$  on  $|\Psi\rangle$ .
6   Measure all the  $n$  qubits to compute the probability  $p_k$  of obtaining the state  $|k\rangle$ , for  $k = 0$  to
    $2^n - 1$ .
7    $\delta = \frac{1}{\sqrt{N}}(b_0 - a_0)$ 
8    $\mathbf{u} = [c\sqrt{p_0} - \delta \ c\sqrt{p_1} - \delta \ c\sqrt{p_2} - \delta \ \dots \ c\sqrt{p_{N-1}} - \delta]^T$ 
9   Convert  $\mathbf{u}$  in the sequency order and store it in the vector  $\mathbf{v}$ .
10  return the vector  $\mathbf{v}$ .
```

---

We note that the parameter  $\epsilon$  ensures that Algorithm 1 also works for the special case when the  $\|\tilde{A}\| = 0$ . We already noted that the computational complexity of the classical Fast Walsh-Hadamard Transform [27] for an input vector of size  $N$  is of the order of  $\mathcal{O}(N \log_2 N)$ , whereas our hybrid classical-quantum algorithm (Algorithm 1) for computation of the Walsh-Hadamard transform for an input vector of size  $N$  has a computational complexity of  $\mathcal{O}(N)$ .

## 4 Hybrid Classical-Quantum Algorithms for Image Processing

Two-dimensional Walsh-Hadamard transforms will be needed for image processing applications discussed later in this work. However, before discussing the two-dimensional Walsh-Hadamard transforms, first we recall our the convention that  $x_i \in \{0, 1\}$  denotes the  $i$ -th bit in the binary representation of the integer  $x$ . More explicitly, it means, if  $x = x_0 + x_1 2 + x_2 2^2 + \dots + x_i 2^i + \dots + x_{n-1} 2^{n-1}$ , then  $x_i$  is the  $i$ -th bit in its binary representation. We define ‘bit-wise inner product’ of two  $n$  bits integers  $x$  and  $y$  as  $\langle x, y \rangle := \sum_{i=0}^{n-1} x_i y_i$ . Let  $f$  be a  $N \times N$  matrix, where  $N = 2^n$  for some positive integer  $n$ . The two-dimensional Walsh-Hadamard transform (in the natural or Hadamard order) of the matrix  $f$  is a  $N \times N$  matrix  $F$ , which may be computed as

$$F_{p,q} := \frac{1}{N} \sum_{r=0}^{N-1} \sum_{s=0}^{N-1} f_{r,s} (-1)^{\langle p,r \rangle + \langle q,s \rangle} = \frac{1}{N} \sum_{r=0}^{N-1} \sum_{s=0}^{N-1} f_{r,s} (-1)^{\sum_{i=0}^{n-1} p_i r_i + q_i s_i}. \quad (4.1)$$

The two-dimensional Walsh-Hadamard inverse transform (in the natural or Hadamard order) of the matrix  $F$  is given by

$$f_{r,s} = \frac{1}{N} \sum_{p=0}^{N-1} \sum_{q=0}^{N-1} F_{p,q} (-1)^{\langle p,r \rangle + \langle q,s \rangle}. \quad (4.2)$$

The normalizing constant  $\frac{1}{N}$  used in Eq. (4.3) and Eq. (4.2) makes the definition of direct and inverse two-dimensional Walsh-Hadamard transforms symmetric.

One can rewrite Eq. (4.3) as

$$F_{p,q} = \frac{1}{N} \sum_{r=0}^{N-1} \left( \sum_{s=0}^{N-1} f_{r,s} (-1)^{\sum_0^{n-1} p_i r_i} \right) (-1)^{\sum_0^{n-1} q_i s_i}. \quad (4.3)$$

It is easy to see that the two-dimensional Walsh-Hadamard transforms of a  $N \times N$  matrix can be carried out in two steps. In the first step the one-dimensional Walsh-Hadamard transforms of all the columns are computed (one column at a time), and then in the second step the one-dimensional Walsh-Hadamard transforms of all the rows are computed. Similarly, The two-dimensional Walsh-Hadamard inverse transform can be implemented as a sequence of two one-dimensional Walsh-Hadamard transforms. For simplicity, we discussed the two-dimensional Walsh-Hadamard transform of an  $N \times N$  matrix. Similarly, the two-dimensional Walsh-Hadamard transforms of an  $N_1 \times N_2$  matrix (where  $N_1$  and  $N_2$  are powers of 2) can be carried out in two steps, by first computing the one-dimensional Walsh-Hadamard transforms of all the columns and then computing the one-dimensional Walsh-Hadamard transforms of all the rows. Using Algorithm 1, the cost for computing the one-dimensional Walsh-Hadamard transform of each column (or row) is  $\mathcal{O}(N_1)$  (or  $\mathcal{O}(N_2)$ ). Therefore, on taking into account the cost of computing the one-dimensional Walsh-Hadamard transforms of  $N_1$  rows and  $N_2$  columns, the total computational cost for computing the two-dimensional Walsh-Hadamard transform of an  $N_1 \times N_2$  matrix (using our proposed approach, also outlined in Algorithm 2) turns out to be  $\mathcal{O}(2N_1N_2) = \mathcal{O}(N_1N_2)$ . This cost is considerably less than the cost of obtaining the two-dimensional Walsh-Hadamard transforms of an  $N_1 \times N_2$  matrix using the classical Fast Walsh-Hadamard transform that has a cost of  $\mathcal{O}(N_1N_2 \log_2 N_1N_2)$ . More generally, it is easy to see that the cost of carrying out  $d$ -dimensional Walsh-Hadamard transform as defined in Eq. (4.4), using the proposed approach is  $\mathcal{O}(\prod_{k=1}^d N_k)$ . In contrast, the cost of obtaining the same result using the classical Fast Walsh-Hadamard transform is  $\mathcal{O}(\prod_{k=1}^d N_k \log_2(\prod_{k=1}^d N_k))$ .

Algorithm 2 computes the two-dimensional Walsh-Hadamard transform of an  $N \times N$  matrix using the approach described above.

---

**Algorithm 2:** A hybrid classical-quantum algorithm for computing two-dimensional Walsh-Hadamard transform.

---

**Input:** A  $N \times N$  matrix  $X$ . Here  $N = 2^n$  for some positive integer  $n$ .

**Output:** The two-dimensional Walsh-Hadamard transform of  $X$ .

*/\* The algorithm uses the quantum subroutine  $\mathcal{H}_Q(\mathbf{v})$  to compute the quantum Walsh-Hadamard transform of the input vector  $\mathbf{v}$  of size  $n$ . \*/*

```

1 Function  $\mathcal{H}_Q^{\otimes 2}(X)$ 
2   for  $j \leftarrow 1$  to  $N$  do
3      $X[j] = \mathcal{H}_Q(X[j])$            // Replace the  $j^{\text{th}}$  column of  $X$  with its Walsh-Hadamard transform.
4   for  $i \leftarrow 1$  to  $N$  do
5      $X^T[i] = \mathcal{H}_Q(X^T[i])$        // Replace the  $i^{\text{th}}$  row of  $X$  with its Walsh-Hadamard transform.
6   return  $X$ .
```

---

**Remark 4.0.1.**

- i. In Algorithm 2, the result of carrying out the one-dimensional Walsh-Hadamard transforms of a column/row is retrieved back and stored classically. The only quantum step in this algorithm involves the subroutine  $\mathcal{H}_Q(\mathbf{v})$  requiring  $n = \log_2 N$  qubits on a quantum computer. It means only  $n = \log_2 N$  qubits are needed for the computation of the two-dimensional Walsh-Hadamard transforms using Algorithm 2.
- ii. For computing the two-dimensional Walsh-Hadamard transforms, all the required one-dimensional Walsh-Hadamard transforms for columns (or rows) may be performed in parallel, but the total number of qubits required would be more.
- iii. We considered two-dimensional Walsh-Hadamard transforms above. It can easily be generalized to higher dimensions. Let  $N_k = 2^{n_k}$ ,  $k = 1, \dots, d$ , then the  $d$ -dimensional Walsh-Hadamard transform (in the natural or Hadamard order) may be computed as

$$F_{p_1, p_2, \dots, p_d} = \frac{1}{\left(\prod_{k=1}^d \sqrt{N_k}\right)} \sum_{r_1=0}^{N_1-1} \sum_{r_2=0}^{N_2-1} \dots \sum_{r_d=0}^{N_d-1} f_{r_1, r_2, \dots, r_d} (-1)^{\sum_{k=1}^d \langle p_k, r_k \rangle}. \quad (4.4)$$

Here,  $0 \leq p_k, r_k \leq N_k - 1$  and  $\langle p_k, r_k \rangle = \sum_{i=0}^{n_k-1} p_{k,i} r_{k,i}$  with  $p_{k,i}$  and  $r_{k,i}$  denoting the  $i$ -th bit in the binary representation of the integer  $p_k$  and  $r_k$ , respectively.

- iv. As discussed earlier, the computational cost associated with obtaining the 2-dimensional Walsh-Hadamard transform using the proposed hybrid approach (outlined in Algorithm 2) is  $\mathcal{O}(N_1 N_2)$ . This estimate includes classical and quantum components. The classical component including state preparation, scaling, shifting and measurement/retrieval operations has a cost of  $\mathcal{O}(N_1 N_2)$ . The quantum component involving the quantum Walsh-Hadamard transform has a cost of  $\mathcal{O}(1)$ .

For image processing applications, the Walsh-Hadamard transform in the sequency order is preferred because of its superior energy compaction properties in comparison to the Walsh-Hadamard transform in the natural order. We describe below quick methods of converting from one ordering of the Walsh-Hadamard transformed vector to the other.

The ordering index in the natural order can be computed by reversing the bits of the gray code representation of the ordering index in the sequency order. Suppose  $s$  is the ordering index in the sequency order and one needs to obtain the corresponding ordering index  $h$  in the natural order. Then the first step is to compute the bits of the gray code  $g$  for  $s$  as follows.

$$\begin{aligned} g_{n-1} &= s_{n-1}, \\ g_i &= s_i \oplus s_{i+1} \quad \text{for } i = 0, 1, 2, \dots, n-2. \end{aligned}$$

Here,  $\oplus$  denotes the bitwise XOR operation (or equivalently addition modulo 2). Once  $g$  is known,  $h$  is obtained by simply reversing the bits of  $g$ , i.e.  $h_i = g_{n-1-i}$  for  $i = 0, 1, 2, \dots, n-1$ . Next, suppose ordering index  $h$  in the natural order is known. Then the corresponding ordering index in the sequency order is obtained as follows. First, the bits of  $h$  are reversed to obtain  $g$ . It means,  $g_i = h_{n-1-i}$  for  $i = 0, 1, 2, \dots, n-1$ . Then  $s$  is obtained by the following computation.

$$\begin{aligned} s_{n-1} &= g_{n-1}, \\ s_i &= g_i \oplus s_{i+1} \quad \text{for } i = n-2, \dots, 2, 1, 0. \end{aligned}$$

## 5 Computational Examples

In this section, we will give computational examples to illustrate the application of the two-dimensional Walsh-Hadamard transforms in image processing using our hybrid classical-quantum approach. The computation of the two-dimensional Walsh-Hadamard transforms using our hybrid classical-quantum approach yields computational advantages in comparison to a purely classical algorithm. Therefore, although the examples considered in this section can be implemented using a purely classical algorithm, they would be less efficient than our proposed method (see Sec. 4).

In the following first we describe an algorithm for image filtering (Algorithm 3), which involves the suppression of high frequency components, and then provide relevant computational examples. Subsequently, we describe algorithms for removing periodic banding noise from a given image. The cases involving images with the vertical banding noise, the horizontal banding noise and the combined horizontal and vertical banding noise will be considered. We note that the proposed algorithms for image filtering were successfully implemented and tested using the simulated environment of Qiskit (IBM's open source quantum computing platform).

### 5.1 Example 1 - Image Filtering

Image filtering is a very common digital image processing technique used to suppress the noise in the image and make the image smooth. Noise is undesirable as it degrades the quality of the image. The source of noise could be the camera sensor itself or the noise could get introduced during the electronic transmission of the image. The Walsh-Hadamard transform can be used for image filtering in the frequency domain. Suppose  $A$  is the  $N \times N$  matrix representing the gray scale input image to be filtered. Then the first step in image filtering using the Walsh-Hadamard transform method is to carry out the 2-dimensional Walsh-Hadamard transform of  $A$  to get the transformed image  $\tilde{A}$  in the frequency domain. Next, the image is filtered in the frequency domain. A simple filtering scheme involves suppressing certain high or low frequency components as needed. More complex filters using convolution may be used at this step depending on the requirement. Finally, the image is converted back to the spatial domain by performing the 2-dimensional inverse Walsh-Hadamard transform.

From the above discussion, we get the following algorithm for image filtering which involves the suppression of high frequency components.

---

**Algorithm 3:** A hybrid classical-quantum algorithm for image filtering.

---

**Input:** A  $N \times N$  matrix  $X$  corresponding to the gray scale image to be filtered. Here  $N = 2^n$  for some positive integer  $n$ .

**Output:** A filtered version of  $X$ , with the right bottom  $r \times r$  frequency block suppressed.

```

/* The algorithm uses the quantum subroutine  $\mathcal{H}_Q(\mathbf{v})$  to compute the quantum Walsh-Hadamard transform of
the input vector  $\mathbf{v}$ . */
1  $X = \mathcal{H}_Q^{\otimes 2}(X)$  // Compute the two-dimensional Walsh-Hadamard transform of  $X$  using Algorithm 2.
2 for  $i \leftarrow N - r$  to  $N$  do
3   for  $j \leftarrow N - r$  to  $N$  do
4      $X[i][j] = 0$  // Suppress the right bottom  $r \times r$  frequency block.
5  $X = \mathcal{H}_Q^{\otimes 2}(X)$  // Compute the two-dimensional inverse Walsh-Hadamard transform of  $X$  using Algorithm 2.
6 return  $X$ .
```

---

The filtering of an image by suppressing the high frequency components is illustrated in Fig. 1. The original  $n \times n$  image (where  $n = 512$ ) is shown in Fig. 1 (a). This image is transformed to the frequency domain by carrying out the 2-dimensional Walsh-Hadamard transform. In the frequency domain the elements of the submatrix  $\tilde{A}(n-r : n-r)$  are set to 0. Here  $\tilde{A}(n-r : n-r)$  denotes the right bottom  $r \times r$  block of the  $n \times n$  matrix. It means all the entries in this high frequency  $r \times r$  block is set to 0. Then by performing the 2-dimensional inverse Walsh-Hadamard transform the image is converted back to the spatial domain. In Fig. 1 (b), (c), (d), (e) and (f), the size of suppressed frequency blocks are  $r \times r$  where  $r = 256, 384, 448, 480,$  and  $496$  respectively.

Clearly, if too few frequency components are retained, then the quality of the image gets degraded. We recall some typical quality metrics used in digital image processing applications.

- Mean Squared Error (MSE) between two images  $f(x, y)$  and  $g(x, y)$  of size  $M \times N$  is defined as

$$MSE(f, g) = \frac{1}{MN} \sum_{m=0}^M \sum_{n=0}^N (f(m, n) - g(m, n))^2.$$

- Peak Signal to Noise Ratio (PSNR) for two images  $f(x, y)$  and  $g(x, y)$  of size  $M \times N$  is defined as

$$PSNR(f, g) = 10 \log_{10} \left( \frac{M^2}{MSE(f, g)} \right),$$

where  $M$  is the peak value (i.e., the maximum value) in the image data. For grey-level (8 bits) images  $M$  is 255. Clearly, as the  $MSE(f, g)$  approaches zero, the  $PSNR(f, g)$  approaches infinity.

- Structure Similarity Index Method (SSIM) is used to measure the similarity between two images based on the luminance, contrast and structural correlations. This metric is very close to the human perception of similarity between two images, [28]. It is defined as

$$SSIM(f, g) = l(x, y) c(x, y) s(x, y),$$

where

$$\begin{aligned} l(f, g) &= \frac{2\mu_f \mu_g + C_1}{\mu_f^2 + \mu_g^2 + C_1} \\ c(f, g) &= \frac{2\sigma_f \sigma_g + C_2}{\sigma_f^2 + \sigma_g^2 + C_2} \\ s(f, g) &= \frac{\sigma_{fg} + C_3}{\sigma_f \sigma_g + C_3}. \end{aligned}$$

We note that for two images  $f$  and  $g$ , the function  $l(f, g)$  captures the similarity in mean luminance ( $\mu$  denotes mean). The function  $c(f, g)$  measures the closeness in contrast ( $\sigma$  denotes standard deviation) and the function  $s(f, g)$  gives the structural similarity between the two images  $f$  and  $g$  ( $\sigma_{fg}$  denotes covariance between  $f$  and  $g$ ).

Table 1 below describes how the quality of the filtered image depends on the size of the suppressed block in the frequency domain.

The same approach can be used for filtering of color images via the application of the above algorithm for each of the RGB (Red, Green and Blue) channels. The original image of size  $512 \times 512$  is shown in

Figure	Size of the suppressed block	MSE	PSNR	SSIM	Image size
1 (a)	$0 \times 0$	0	0	$\infty$	258 KB
1 (b)	$256 \times 256$	4.32	0.98	41.77	252 KB
1 (c)	$384 \times 384$	18.83	35.38	0.91	228 KB
1 (d)	$448 \times 448$	48	31.32	0.82	196 KB
1 (e)	$480 \times 480$	96.14	28.30	0.73	167 KB
1 (f)	$496 \times 496$	164.13	25.98	0.66	143 KB

Table 1: Quality parameters of the filtered image.

Fig. 2 (a). Fig. 2 (b) and (c) are obtained by suppressing sequency blocks as discussed earlier. The size of suppressed sequency block is  $480 \times 480$  for Fig. 2 (b) and  $448 \times 448$  for Fig. 2 (c). We note that even after suppressing sequency block of size  $448 \times 448$ , with naked eye the resulting image shown Fig. 2 (c) appears as good as the original image in Fig. 2 (a).

## 5.2 Example 2 - Periodic Banding Noise Removal

As our next example, we take up the removal of periodic banding noise using the Walsh-Hadamard transform approach. Such periodic banding noise is known to occur in digital photography and image capturing, for example in satellite images associated with differences between the forward and reverse scans of the sensor [29].

### 5.2.1 Periodic Vertical Banding Noise

The image in Fig. 3(a) contains a vertical periodic banding noise. A hybrid classical-quantum approach for removing this vertical periodic banding noise is described in Algorithm 4. We note that Algorithm 4 begins by computing the 2-dimensional Walsh-Hadamard transform of the matrix representing the noisy image. Then the key step in Algorithm 4 is to suppress all the elements (i.e., the sequency components) in the first row except the first element in the first row of the transformed matrix (see Step 3 in Algorithm 4). Finally, the 2-dimensional inverse Walsh-Hadamard transform is carried out to get back the filtered image with the vertical periodic banding noise removed. The result of applying Algorithm 4 to the noisy image shown in Fig. 3(a) results in the image in Fig. 3(b). It is clear that the image in Fig. 3(b) is mostly free of the periodic



(a) Original image, Size:  $512 \times 512$ .



(b) MSE: 4.32, SSIM: 0.98, PSNR: 41.77, SSB:  $256 \times 256$ .



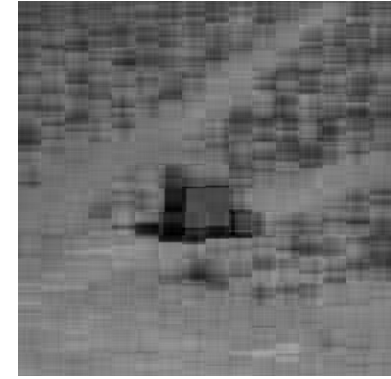
(c) MSE: 18.83, SSIM: 0.91, PSNR: 35.38, SSB:  $384 \times 384$ .



(d) MSE: 48, SSIM: 0.82, PSNR: 31.32, SSB:  $448 \times 448$ .



(e) MSE: 96.14, SSIM: 0.73, PSNR: 28.30, SSB:  $480 \times 480$ .



(f) MSE: 164.13, SSIM: 0.66, PSNR: 25.98, SSB:  $496 \times 496$ .

Figure 1: Image filtering by suppressing high frequency signals. SSB denotes the size of the suppressed frequency block.

vertical banding noise present in the input image Fig. 3(a).

---

**Algorithm 4:** A hybrid classical-quantum algorithm for the removal of vertical banding noise.

---

**Input:** A  $N \times N$  matrix  $X$  corresponding to the gray scale. The image contains a vertical band noise which needs to be filtered. Here  $N = 2^n$  for some positive integer  $n$ .

**Output:** A filtered version of  $X$  with the vertical band noise removed.

```

/* The algorithm uses the quantum subroutine  $\mathcal{H}_Q(\mathbf{v})$  to compute the quantum Walsh-Hadamard transform of
the input vector  $\mathbf{v}$ . */
1  $X = \mathcal{H}_Q^{\otimes 2}(X)$  // Compute the two-dimensional Walsh-Hadamard transform of  $X$  using Algorithm 2.
2 for  $j \leftarrow 2$  to  $N$  do
3    $X[1][j] = 0$  // Suppress all but the first element in the first row in the sequency domain
4  $X = \mathcal{H}_Q^{\otimes 2}(X)$  // Compute the two-dimensional inverse Walsh-Hadamard transform of  $X$  using Algorithm 2.
5 return  $X$ .
```

---

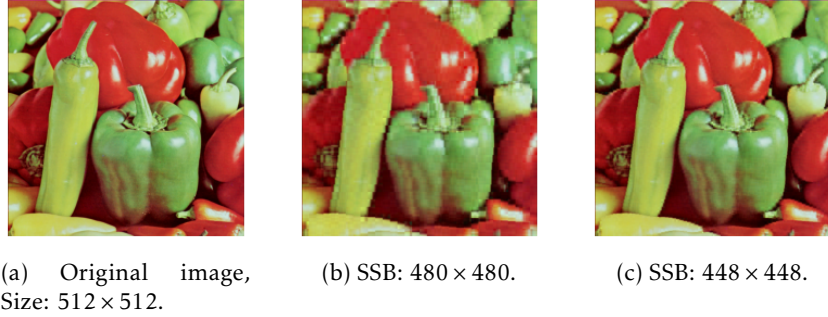


Figure 2: Image filtering by suppressing high frequency signals for each of the RGB channels of a colored image. SSB denotes the size of the suppressed frequency block.

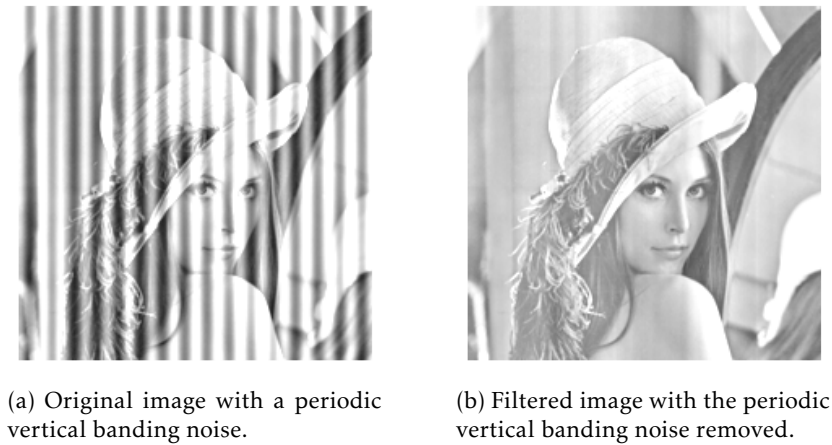


Figure 3: Vertical banding noise removal.

### 5.2.2 Periodic Horizontal Banding Noise

Next, we consider an image, Fig. 4(a), containing horizontal periodic banding noise. The method of removing this noise is quite similar to the approach in Algorithm 4. The only change needed in Algorithm 4 is to modify Step 3 such that instead of suppressing elements in the first row (except the first element) in the frequency domain, elements in the first column (except the first element) in frequency domain are suppressed. The image in Fig. 4(b) shows the resulting image after the removal of horizontal periodic banding noise from Fig. 4(a).

### 5.2.3 Combined Horizontal and Vertical Banding Noise

Suppose an image contains both the horizontal and the vertical periodic banding noise as in Fig. 5(a). By suppressing elements in the first column and also the elements in the first row (except the element at the position  $(1, 1)$ , i.e. the top left element) in the transformed matrix in the frequency domain, one can remove both the vertical periodic banding noise from Fig. 5(a). The method is described in detail in Algorithm 5. The ‘offset’ value in Algorithm 5 controls the intensity of the filtered image. The resulting filtered image

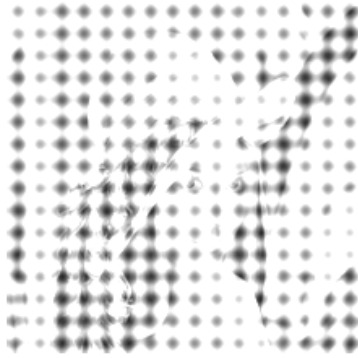


(a) Original image with a periodic horizontal banding noise.



(b) Filtered image with the periodic horizontal banding noise removed.

Figure 4: Horizontal banding noise removal.



(a) Original image with both horizontal and vertical banding noise.



(b) Filtered image with both the horizontal and vertical banding noise removed.

Figure 5: Both horizontal and vertical banding noise removal.

with the 'offset' value 150 in Algorithm 5 is shown in Fig. 5(b).

---

**Algorithm 5:** A hybrid classical-quantum algorithm for the removal of combined horizontal and vertical banding noise.

---

**Input:** A  $N \times N$  matrix  $X$  corresponding to the gray scale. The image contains a vertical band noise which needs to be filtered. Here  $N = 2^n$  for some positive integer  $n$ .

**Output:** A filtered version of  $X$  with the vertical band noise removed.

```

/* The algorithm uses the quantum subroutine  $\mathcal{H}_Q(\mathbf{v})$  to compute the quantum Walsh-Hadamard transform of
the input vector  $\mathbf{v}$ .                                                                                                     */
1  $X = \mathcal{H}_Q^{\otimes 2}(X)$  // Compute the two-dimensional Walsh-Hadamard transform of  $X$ .
2 for  $j \leftarrow 2$  to  $N$  do
3    $X[1][j] = 0$  // Suppress all but the first element in the first row in the sequency domain
4    $X[j][1] = 0$  // Suppress all but the first element in the first column in the sequency domain
5  $X[1][1] = N \times \text{offset}$  // The 'offset' value controls the intensity of the filtered image.
6  $X = \mathcal{H}_Q^{\otimes 2}(X)$  // Compute the two-dimensional inverse Walsh-Hadamard transform of  $X$ .
7 return  $X$ .
```

---

## 6 Conclusion

In this work, we proposed a hybrid classical-quantum approach for obtaining multi-dimensional Walsh-Hadamard transforms of arbitrary real fields with applications to quantum image processing. These multi-dimensional Walsh-Hadamard transforms are obtained using quantum Hadamard gates (along with state-preparation, shifting, scaling and measurement operations) and can be considered as generalization of evaluation of one-dimensional Walsh-Hadamard transforms of arbitrary vectors presented in a recent work [8]. Our proposed approach makes efficient use of qubits as it needs only  $\log_2 N$  qubits for sequential processing of an image of  $N \times N$  pixels. This representation can be considered to more efficient, when compared to many other commonly used quantum image representations discussed in the literature. This becomes an important advantage especially considering the scarcity of available qubits in current generation of quantum computers.

We note that the computational cost of the proposed approach for the computation of a  $d$ -dimensional Walsh-Hadamard transform, as defined in Eq. (4.4), is considerably lower (with  $\mathcal{O}(\prod_{k=1}^d N_k)$  operations) compared to the classical Fast Walsh-Hadamard transform (with  $\mathcal{O}(\prod_{k=1}^d N_k \log_2(\prod_{k=1}^d N_k))$  operations). The proposed approach for obtaining the Walsh-Hadamard transform of image data (where  $d = 2$ ) was implemented and tested on the simulation environment on Qiskit (IBM's open source quantum computing platform). Applications of the proposed approach were successfully demonstrated via computational examples relevant to basic image filtering and periodic banding noise removal. Future work could involve applications of the core methodology proposed here to image, video and/or high-dimensional data compression.

## References

- [1] Peter W Shor. Algorithms for quantum computation: discrete logarithms and factoring. In Proceedings 35th annual symposium on foundations of computer science, pages 124–134. Ieee, 1994.
- [2] Peter W Shor. Polynomial-time algorithms for prime factorization and discrete logarithms on a quantum computer. SIAM review, 41(2):303–332, 1999.
- [3] Lov K Grover. A Fast Quantum Mechanical Algorithm for Database Search. In Proceedings of the Twenty-eighth Annual ACM Symposium on Theory of Computing, pages 212–219. ACM, 1996.
- [4] Lov K Grover. Quantum mechanics helps in searching for a needle in a haystack. Physical review letters, 79(2):325, 1997.
- [5] Aram W Harrow, Avinatan Hassidim, and Seth Lloyd. Quantum algorithm for linear systems of equations. Physical review letters, 103(15):150502, 2009.
- [6] Dominic W Berry. High-order quantum algorithm for solving linear differential equations. Journal of Physics A: Mathematical and Theoretical, 47(10):105301, 2014.
- [7] Edward Farhi, Jeffrey Goldstone, and Sam Gutmann. A quantum approximate optimization algorithm. arXiv preprint [arXiv:1411.4028](https://arxiv.org/abs/1411.4028), 2014.
- [8] Alok Shukla and Prakash Vedula. A hybrid classical-quantum algorithm for solution of nonlinear ordinary differential equations. arXiv preprint [arXiv:2112.00602](https://arxiv.org/abs/2112.00602), 2021.

- [9] Peter Wittek. Quantum machine learning: what quantum computing means to data mining. Academic Press, 2014.
- [10] Zhaobin Wang, Minzhe Xu, and Yaonan Zhang. Review of quantum image processing. Archives of Computational Methods in Engineering, pages 1–25.
- [11] Xi-Wei Yao, Hengyan Wang, Zeyang Liao, Ming-Cheng Chen, Jian Pan, Jun Li, Kechao Zhang, Xingcheng Lin, Zhehui Wang, Zhihuang Luo, et al. Quantum image processing and its application to edge detection: theory and experiment. Physical Review X, 7(3):031041.
- [12] Yue Ruan, Xiling Xue, and Yuanxia Shen. Quantum image processing: opportunities and challenges. Mathematical Problems in Engineering, 2021.
- [13] Suzhen Yuan, Xuefeng Mao, Jing Zhou, and Xiaofa Wang. Quantum image filtering in the spatial domain. International Journal of Theoretical Physics, 56(8):2495–2511, 2017.
- [14] Fei Yan, Abdullah M Iliyasu, and Salvador E Venegas-Andraca. A survey of quantum image representations. Quantum Information Processing, 15(1):1–35.
- [15] Yue Ruan, Hanwu Chen, Zhihao Liu, and Jianing Tan. Quantum image with high retrieval performance. Quantum Information Processing, 15(2):637–650.
- [16] Kenneth George Beauchamp. Walsh functions and their applications. Academic Press, 1975.
- [17] Michael A. Nielsen and Isaac Chuang. Quantum Computation and Quantum Information. Cambridge University Press, 2000.
- [18] WS Kuklinski. Fast Walsh transform data-compression algorithm: ECG applications. Medical and Biological Engineering and Computing, 21(4):465–472, 1983.
- [19] C Zarowski and Maurice Yunik. Spectral filtering using the fast Walsh transform. IEEE transactions on acoustics, speech, and signal processing, 33(5):1246–1252, 1985.
- [20] Tom Beer. Walsh transforms. American Journal of Physics, 49(5):466–472, 1981.
- [21] Henry F Ahner. Walsh functions and the solution of nonlinear differential equations. American Journal of Physics, 56(7):628–633, 1988.
- [22] Peter A Gnoffo. Global series solutions of nonlinear differential equations with shocks using Walsh functions. Journal of Computational physics, 258:650–688, 2014.
- [23] Peter A Gnoffo. Unsteady solutions of non-linear differential equations using Walsh function series. In 22nd AIAA Computational Fluid Dynamics Conference, page 2756, 2015.
- [24] Peter A Gnoffo. Solutions of nonlinear differential equations with feature detection using fast Walsh transforms. Journal of Computational Physics, 338:620–649, 2017.
- [25] CF Chen and CH Hsiao. A Walsh series direct method for solving variational problems. Journal of the Franklin Institute, 300(4):265–280, 1975.
- [26] Yi Lu and Yvo Desmedt. Walsh transforms and cryptographic applications in bias computing. Cryptography and Communications, 8(3):435–453, 2016.

- [27] Youssef A. Geadah and MJG Corinthios. Natural, dyadic, and sequency order algorithms and processors for the Walsh-hadamard transform. IEEE Transactions on Computers, 26(05):435–442, 1977.
- [28] Zhou Wang, A.C. Bovik, H.R. Sheikh, and E.P. Simoncelli. Image quality assessment: from error visibility to structural similarity. IEEE Transactions on Image Processing, 13(4):600–612, 2004.
- [29] Bruce K Quirk. A technique for the reduction of banding in Landsat Thematic Mapper images. Photogrammetric Engineering & Remote Sensing, 58(10):1425–1431, 1992.